

Josephson Current through a Planar Junction of Graphene

Yositake TAKANE and Ken-Ichiro IMURA

*Department of Quantum Matter, Graduate School of Advanced Sciences of Matter,
Hiroshima University, Higashihiroshima, Hiroshima 739-8530, Japan*

(Received)

Josephson effect in a planar graphene junction is studied by assuming that the coupling of a graphene sheet and two superconductors deposited on its top is described by a tunneling Hamiltonian. This model properly takes account of the proximity effect characteristic to a planar junction, and allows us to treat monolayer and bilayer cases in a parallel manner. Applying a quasiclassical Green's function approach to it we analyze the Josephson critical current I_c in a short-junction limit. As a characteristic feature of the planar junction we find that I_c is a concave function of temperature at the strong coupling limit while it crosses over to a convex function with decreasing the coupling strength. We also find different chemical-potential dependences of I_c in the monolayer and bilayer cases.

KEYWORDS: Josephson effect, monolayer graphene, bilayer graphene, quasiclassical Green's function

Since the realization of a monolayer sheet of graphene,¹⁾ extensive studies have been devoted to uncovering unusual electronic properties of this material.²⁾ Josephson effect in graphene has been a target of intense theoretical³⁻⁹⁾ and experimental¹⁰⁻¹³⁾ studies during the last few years. The main interest is focused on how the Josephson current is affected by the unique band structure of graphene, i.e., the conduction and valence bands touch conically at K_+ and K_- points in the Brillouin zone, and the density of states vanishes at the energy of the band touching point (i.e., Dirac point), which is set as $\epsilon = 0$ hereafter. Titov and Beenakker⁴⁾ calculated the Josephson current through a monolayer graphene sheet on which two superconducting electrodes are deposited with separation L , under the assumption that carriers are heavily doped in the region covered by the superconductors. In the short-junction limit where L is much shorter than the superconducting coherence length ξ , they obtained the critical current I_c at zero temperature as a function of the chemical potential μ . It is shown that I_c is finite even at $\mu = 0$ and linearly increases with increasing μ . An experimental result consistent with this prediction has been reported.¹⁰⁾

We focus on another interesting aspect of the Josephson effect in graphene, stemming from the fact that graphene is a unique realization of an isolated ideal two-dimensional (2D) electron

system. Graphene in a Josephson junction acquires a 2D (planar) contact with a superconductor, since a natural way to create a superconductor-graphene-superconductor junction is to deposit superconducting electrodes on top of a graphene flake.^{10–13)} This is quite contrasting to the case of a usual 2D electron gas imbedded in a semiconductor hetero-structure that has a one-dimensional (linear) contact with superconducting electrodes. However, the previous theoretical studies have not paid attention to the structure of such a planar junction. In the model used so far,^{4,5,7,9)} an energy-independent effective pair potential Δ_G is induced inside the graphene sheet over the region covered by the superconductors. This assumption reduces the planar junction to a conventional linear junction model. It is questionable whether the superconducting proximity effect in a planar junction is fully described by a conventional model with Δ_G .

In this letter we study the stationary Josephson effect in the planar junction of graphene by employing a simple model in which a graphene sheet is coupled with superconductors by a tunneling Hamiltonian.¹⁴⁾ This model properly describes the proximity effect characteristic to a planar junction, which is ignored in the previous theoretical studies, allowing us to treat monolayer and bilayer cases in a parallel manner. We apply a quasiclassical Green's function approach^{15,16)} to our model under an effective mass approximation.¹⁷⁾ When μ is away from the Dirac point, our approach enables us to derive a general expression for the Josephson current, which is applicable for an arbitrary coupling strength Γ between the graphene sheet and the superconductors. Using this expression we calculate the Josephson current in the short-junction limit. We show that I_c is a concave function of temperature T at the large- Γ limit, while it crosses over to a convex function with decreasing Γ . This convex T -dependence was not observed in the previous study⁹⁾ based on the model with an energy-independent effective pair potential, and should be regarded as a characteristic feature of the planar junction. We also show that the μ -dependence of I_c at $T = 0$ qualitatively differs in the monolayer and bilayer cases. We set $k_B = \hbar = 1$ throughout this letter.

Let us consider a clean graphene sheet on which two superconductors, S_1 and S_2 , of width W are deposited with separation L , where S_1 and S_2 occupy the region of $L/2 \leq x$ and that of $x \leq -L/2$, respectively (see Fig. 1). Note that only the top layer is in contact with S_1 and S_2 in the bilayer case. Under the condition of $W \gg L$, we regard our system as being translationally invariant in the y -direction. We assume that carrier doping is uniform in graphene and that the pair potential $\Delta(x)$ for the superconductors is given by $\Delta(x) = \Delta e^{i\varphi/2}$ in S_1 and $\Delta e^{-i\varphi/2}$ in S_2 . We use a tunneling Hamiltonian to describe the coupling of the graphene sheet and the superconductors. The resulting proximity effect on quasiparticles

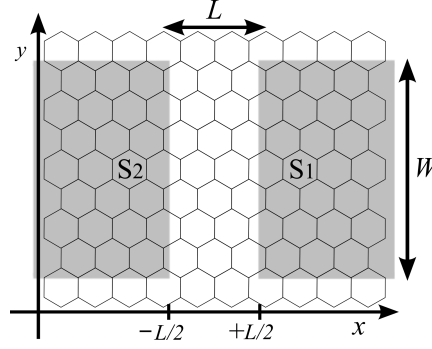


Fig. 1. Planar junction geometry: Josephson junction consisting of a graphene sheet on which two superconductors S_1 and S_2 of width W are deposited with separation L . The pair potential is assumed to be $\Delta e^{i\varphi/2}$ in S_1 and $\Delta e^{-i\varphi/2}$ in S_2 .

in graphene is described by a self-energy¹⁴⁾ for the thermal Green's function given below. We consider only quasiparticle states near the K_+ point because the K_+ and K_- points are degenerate. To describe quasiparticle states in graphene on the basis of a tight-binding model,^{17,18)} we introduce nearest-neighbor transfer integral γ_0 . In addition, we employ nearest-neighbor interlayer coupling γ_1 and next nearest-neighbor interlayer coupling γ_3 in the bilayer case. They are estimated as $\gamma_0 \approx 2.8$ eV, $\gamma_1 \approx 0.4$ eV, and $\gamma_3 \approx 0.3$ eV.²⁾ Let us introduce the thermal Green's function $\check{G}_j(\mathbf{r}, \mathbf{r}'; \omega_n)$ with the Matsubara frequency $\omega_n = (2n + 1)\pi T$. The subscript $j = 1$ ($j = 2$) specifies the monolayer (bilayer) case. Within an effective mass approximation, the Green's function obeys

$$(i\omega_n \check{\tau}_{4 \times 4}^z - \check{H}_j - \check{\Sigma}_j) \check{G}_j(\mathbf{r}, \mathbf{r}'; \omega_n) = \check{\tau}_{4 \times 4}^0 \delta(\mathbf{r} - \mathbf{r}') \quad (1)$$

with $\check{\tau}_{4 \times 4}^z = \text{diag}(1, 1, -1, -1)$, $\check{\tau}_{4 \times 4}^0 = \text{diag}(1, 1, 1, 1)$, $\check{H}_j = \text{diag}(H_j, H_j)$. The 2×2 effective Hamiltonian H_j for low-energy quasiparticles is given by

$$H_1 = \begin{pmatrix} -\mu & \gamma \hat{k}_- \\ \gamma \hat{k}_+ & -\mu \end{pmatrix} \quad (2)$$

for the monolayer case¹⁷⁾ with $\gamma = (\sqrt{3}/2)\gamma_0 a$ (a : lattice constant) and $\hat{k}_\pm = -i\partial_x \pm \partial_y$, and

$$H_2 = \begin{pmatrix} -\mu & -\alpha \hat{k}_+^2 - \beta \hat{k}_- \\ -\alpha \hat{k}_-^2 - \beta \hat{k}_+ & -\mu \end{pmatrix} \quad (3)$$

for the bilayer case¹⁹⁾ with $\alpha = \gamma^2/\gamma_1$ and $\beta = (\sqrt{3}/2)\gamma_3 a$ characterizing the trigonal warping. The self-energy $\check{\Sigma}_j$ is given by¹⁴⁾

$$\check{\Sigma}_j = \frac{-i\Gamma}{\sqrt{\Delta^2 + \omega_n^2}} \begin{pmatrix} \omega_n \chi_{2 \times 2}^{(j)} & \Delta(x) \chi_{2 \times 2}^{(j)} \\ \Delta(x)^* \chi_{2 \times 2}^{(j)} & -\omega_n \chi_{2 \times 2}^{(j)} \end{pmatrix} \theta(|x| - L/2), \quad (4)$$

where Γ characterizes the coupling strength between the graphene sheet and the superconductors, $\chi_{2 \times 2}^{(1)} = \text{diag}(1, 1)$, and $\chi_{2 \times 2}^{(2)} = \text{diag}(1, 0)$. The matrix form of $\chi_{2 \times 2}^{(2)}$ reflects the fact that only the top layer is in contact with the superconductors in the bilayer case.²⁰⁾ The off-diagonal elements of $\check{\Sigma}_j$ are regarded as an energy-dependent effective pair potential, while the diagonal elements describe renormalization of a quasiparticle energy. If the ω_n -dependence is ignored by setting $\omega_n = 0$, our model is reduced to the conventional one.^{4,5,9)}

Hereafter we restrict our attention to the moderate doping regime of $\gamma_0, \gamma_1 \gg \mu \gg \Delta$. To introduce the quasiclassical Green's function, we perform a Fourier transformation as

$$\check{G}_j(\mathbf{p}, \mathbf{r}; \omega_n) = \int d^2s e^{-i\mathbf{p} \cdot \mathbf{s}} \check{G}_j\left(\mathbf{r} + \frac{\mathbf{s}}{2}, \mathbf{r} - \frac{\mathbf{s}}{2}; \omega_n\right), \quad (5)$$

where $\mathbf{p} = (p_x, p_y)$. In the monolayer case of $j = 1$, the Green's function obeys

$$(i\omega_n \check{\tau}_{4 \times 4}^z - \check{\mathcal{H}}_1 - \check{\Sigma}_1) \check{G}_1(\mathbf{p}, \mathbf{r}; \omega_n) = \check{\tau}_{4 \times 4}^0, \quad (6)$$

where the 4×4 Hamiltonian $\check{\mathcal{H}}_1$ is given by $\check{\mathcal{H}}_1 = \text{diag}(\tilde{H}_1 + h_1, \tilde{H}_1 + h_1)$ with

$$\tilde{H}_1 = \begin{pmatrix} -\mu & \gamma(p_x - ip_y) \\ \gamma(p_x + ip_y) & -\mu \end{pmatrix}, \quad (7)$$

$$h_1 = \begin{pmatrix} 0 & \frac{\gamma}{2} \hat{k}_- \\ \frac{\gamma}{2} \hat{k}_+ & 0 \end{pmatrix}. \quad (8)$$

The 2×2 matrix \tilde{H}_1 is diagonalized as $u_{\mathbf{p}}^\dagger \tilde{H}_1 u_{\mathbf{p}} = \text{diag}(\gamma p - \mu, -\gamma p - \mu)$ in terms of

$$u_{\mathbf{p}} = \frac{1}{\sqrt{2}} \begin{pmatrix} 1 & -e^{-i\phi_{\mathbf{p}}} \\ e^{i\phi_{\mathbf{p}}} & 1 \end{pmatrix}, \quad (9)$$

where $p = |\mathbf{p}|$ and $\phi_{\mathbf{p}} = \arg\{p_x + ip_y\}$. As long as $\mu \gg \Delta$, the subband with the energy dispersion $-\gamma p - \mu$ is irrelevant in the superconducting proximity effect. Therefore, we are allowed to consider only the relevant subband with the energy dispersion $\gamma p - \mu$. In accordance with this observation, we transform \check{G}_1 as $\check{\mathcal{G}}_1(\mathbf{p}, \mathbf{r}; \omega_n) = \check{U}_{\mathbf{p}}^\dagger \check{G}_1(\mathbf{p}, \mathbf{r}; \omega_n) \check{U}_{\mathbf{p}}$ with $\check{U}_{\mathbf{p}} = \text{diag}(u_{\mathbf{p}}, u_{\mathbf{p}})$ and retain only the (1,1)-, (1,3)-, (3,1)-, and (3,3)-elements.²⁰⁾ Accordingly, we define G_1 as

$$G_1 = \begin{pmatrix} [\check{\mathcal{G}}_1]_{1,1} & [\check{\mathcal{G}}_1]_{1,3} \\ [\check{\mathcal{G}}_1]_{3,1} & [\check{\mathcal{G}}_1]_{3,3} \end{pmatrix}. \quad (10)$$

The Green's function G_1 approximately satisfies

$$\left[i\omega_n \tau_{2 \times 2}^z - \left(\gamma p - \mu + \frac{i}{2} \mathbf{v}_1(\mathbf{p}) \cdot \nabla \right) - \Sigma_1 \right] G_1(\mathbf{p}, \mathbf{r}; \omega_n) = \tau_{2 \times 2}^0, \quad (11)$$

where $\tau_{2 \times 2}^z = \text{diag}(1, -1)$, $\tau_{2 \times 2}^0 = \text{diag}(1, 1)$, the velocity $\mathbf{v}_1(\mathbf{p})$ is given by $\mathbf{v}_1(\mathbf{p}) =$

$\gamma(\cos \phi_{\mathbf{p}}, \sin \phi_{\mathbf{p}})$, and

$$\Sigma_1 = \frac{-i\Gamma}{\sqrt{\Delta^2 + \omega_n^2}} \begin{pmatrix} \omega_n & \Delta(x) \\ \Delta(x)^* & -\omega_n \end{pmatrix} \theta(|x| - L/2). \quad (12)$$

By repeating the argument similar to this we can show that the Green's function for the bilayer case satisfies

$$\left[i\omega_n \tau_{2 \times 2}^z - \left(\epsilon_{\mathbf{p}} - \mu + \frac{i}{2} \mathbf{v}_2(\mathbf{p}) \cdot \nabla \right) - \Sigma_2 \right] G_2(\mathbf{p}, \mathbf{r}; \omega_n) = \tau_{2 \times 2}^0, \quad (13)$$

where $\epsilon_{\mathbf{p}} = [(\alpha p^2)^2 + 2\alpha\beta p^3 \cos(3\phi_{\mathbf{p}}) + (\beta p)^2]^{1/2}$, and $\Sigma_2 = \Sigma_1/2$. The x - and y -components of $\mathbf{v}_2(\mathbf{p})$ are given by

$$v_{2x}(\mathbf{p}) = 2\alpha p \cos(\theta_{\mathbf{p}} - \phi_{\mathbf{p}}) + \beta \cos \theta_{\mathbf{p}}, \quad (14)$$

$$v_{2y}(\mathbf{p}) = 2\alpha p \sin(\theta_{\mathbf{p}} - \phi_{\mathbf{p}}) - \beta \sin \theta_{\mathbf{p}}, \quad (15)$$

where $\theta_{\mathbf{p}} = \arg\{\alpha p^2 e^{i2\phi_{\mathbf{p}}} + \beta p e^{-i\phi_{\mathbf{p}}}\}$. Note that Σ_2 is smaller by a factor of two than Σ_1 reflecting the fact that only the top layer is in contact with the superconductors.

We define the quasiclassical Green's function $G_j(\mathbf{n}, \mathbf{r}; \omega_n)$ with $\mathbf{n} = \mathbf{p}/p$ as^{21,22)}

$$G_j(\mathbf{n}, \mathbf{r}; \omega_n) = \frac{i}{\pi} \int d\xi_{\mathbf{p}} G_j(\mathbf{p}, \mathbf{r}; \omega_n), \quad (16)$$

where a diverging contribution must be subtracted, and $\xi_{\mathbf{p}} = \gamma p - \mu$ for $j = 1$ and $\xi_{\mathbf{p}} = \epsilon_{\mathbf{p}} - \mu$ for $j = 2$. Applying a standard procedure²²⁾ to eqs. (11) and (13), we can show that the quasiclassical Green's function satisfies

$$i\omega_n [\tau_{2 \times 2}^z, G_j] + i\mathbf{v}_{Fj}(\mathbf{n}) \cdot \nabla G_j - [\Sigma_j, G_j] = 0, \quad (17)$$

where $\mathbf{v}_{Fj}(\mathbf{n})$ represents the Fermi velocity in the momentum direction denoted by \mathbf{n} . We express the elements of $G_j(\mathbf{n}, \mathbf{r}; \omega_n)$ as $[G_j]_{1,1} = -[G_j]_{2,2} = g_j$, $[G_j]_{1,2} = f_j$, and $[G_j]_{2,1} = f_j^\dagger$. Equation (17) yields

$$\mathbf{v}_{Fj}(\mathbf{n}) \cdot \nabla g_j = \zeta_j(x, \omega_n) [\Delta(x)^* f_j - \Delta(x) f_j^\dagger], \quad (18)$$

$$2[1 + \zeta_j(x, \omega_n)] \omega_n f_j + \mathbf{v}_{Fj}(\mathbf{n}) \cdot \nabla f_j = 2\zeta_j(x, \omega_n) \Delta(x) g_j, \quad (19)$$

$$2[1 + \zeta_j(x, \omega_n)] \omega_n f_j^\dagger - \mathbf{v}_{Fj}(\mathbf{n}) \cdot \nabla f_j^\dagger = 2\zeta_j(x, \omega_n) \Delta(x)^* g_j, \quad (20)$$

where

$$\zeta_j(x, \omega_n) = \frac{\Gamma_j}{\sqrt{\Delta^2 + \omega_n^2}} \theta(|x| - L/2) \quad (21)$$

with $\Gamma_1 = \Gamma$ and $\Gamma_2 = \Gamma/2$. Note that although we are considering a Josephson junction of graphene, only the Fermi velocity reflects a feature of graphene in eqs. (18)-(20). We point out that these equations are also applicable to a conventional planar junction of a 2D electron

system.²³⁾

We derive a general expression for the dc Josephson current $I_j(\varphi)$ in terms of the quasiclassical Green's function, where $j = 1$ and 2 correspond to the monolayer and bilayer cases, respectively. We ignore the trigonal warping effect by setting $\beta = 0$. With this simplification, the Fermi velocity is expressed as $\mathbf{v}_{Fj} = v_{Fj}(\cos \phi, \sin \phi)$ with $v_{F1} = \gamma$ and $v_{F2} = 2\gamma\sqrt{\mu/\gamma_1}$. The density of states per spin at the Fermi level is given by $N_1(0) = \mu/(\pi\gamma^2)$ and $N_2(0) = \gamma_1/(2\pi\gamma^2)$, in which the two-fold valley degeneracy is included. The Josephson current is expressed as^{15,16)}

$$I_j(\varphi) = 2\pi e N_j(0) W \int_{-\pi/2}^{\pi/2} \frac{d\phi}{\pi} v_{Fjx} T \sum_{\omega_n} \text{Im} \{g_j(\mathbf{n}, x; \omega_n)\}. \quad (22)$$

Note that in the \mathbf{r} -dependence of g_j , only x is relevant since $W \gg L$ is assumed. Because $I_j(\varphi)$ is independent of x for $|x| \leq L/2$, we evaluate it at $x = L/2$. Parameterizing x as $x = (v_{Fj} \cos \phi)t$, we solve eqs. (18)-(20) with $g_j^2 + f_j f_j^\dagger = 1$ under the boundary condition of

$$\lim_{t \rightarrow \pm\infty} g_j(\mathbf{n}, t; \omega_n) = \frac{\tilde{\omega}}{\tilde{\Omega}}, \quad (23)$$

$$\lim_{t \rightarrow \pm\infty} f_j(\mathbf{n}, t; \omega_n) = \frac{\tilde{\Delta} e^{\pm i\varphi/2}}{\tilde{\Omega}}, \quad (24)$$

where $\tilde{\omega} = [1 + \zeta_j(x, \omega_n)]\omega_n$, $\tilde{\Delta} = \zeta_j(x, \omega_n)\Delta$, and $\tilde{\Omega} = \sqrt{\tilde{\Delta}^2 + \tilde{\omega}^2}$. Note that $x = L/2$ corresponds to $t_+ \equiv L/(2v_{Fj} \cos \phi)$. A straightforward calculation yields

$$g_j(\mathbf{n}, t_+; \omega_n) = \frac{\tilde{\omega}}{\tilde{\Omega}} + \frac{\tilde{\Delta}^2 (\sinh \kappa \cos \frac{\varphi}{2} + i \cosh \kappa \sin \frac{\varphi}{2})}{\tilde{\Omega} (\tilde{\Omega} \cosh \kappa + \tilde{\omega} \sinh \kappa) \cos \frac{\varphi}{2} + i \tilde{\Omega} (\tilde{\Omega} \sinh \kappa + \tilde{\omega} \cosh \kappa) \sin \frac{\varphi}{2}} \quad (25)$$

with $\kappa = \omega_n L / (v_{Fj} \cos \phi)$. We obtain

$$I_j(\varphi) = 2\pi e N_j(0) W \int_{-\pi/2}^{\pi/2} \frac{d\phi}{\pi} v_{Fjx} T \sum_{\omega_n} \frac{\tilde{\Delta}^2 \sin \varphi}{(\tilde{\Omega}^2 + \tilde{\omega}^2) \cosh 2\kappa + 2\tilde{\omega} \tilde{\Omega} \sinh 2\kappa + \tilde{\Delta}^2 \cos \varphi}. \quad (26)$$

Using this general expression one can numerically calculate the Josephson current in the planar junction for arbitrary parameters. In the strong-coupling limit of $\Gamma_j \gg \Delta_0$ with Δ_0 being the magnitude of the pair potential at $T = 0$, eq. (26) is reduced to the ordinary expression for the Josephson current through a 2D electron gas of finite area placed between two superconductors.^{15,24)}

Below we focus on the short-junction limit of $L \ll \xi$, where $\xi \equiv v_{Fj}/(2\pi\Delta_0)$ is the superconducting coherence length, and study the behavior of the critical current for an arbitrary Γ_j . We can approximate as $\cosh 2\kappa \approx 1$ and $\sinh 2\kappa \approx 0$ in the short-junction limit, and obtain

$$I_j(\varphi) = e \mathcal{N}_j T \sum_{\omega_n} \frac{\Gamma_j^2 \Delta^2 \sin \varphi}{\omega_n^2 (\Delta^2 + \omega_n^2 + 2\Gamma_j \sqrt{\Delta^2 + \omega_n^2} + \Gamma_j^2) + \Gamma_j^2 \Delta^2 \cos^2 \frac{\varphi}{2}}, \quad (27)$$

where $\mathcal{N}_j \equiv 2v_{Fj}N_j(0)W$ represents the number of conducting channels. Before considering the critical current, let us observe the behavior of $I_j(\varphi)$ in the strong and weak coupling limits. Firstly we consider the strong coupling limit of $\Gamma_j \gg \Delta_0 \geq \Delta$. In this case we can ignore all terms in the parentheses except for Γ_j^2 , and obtain

$$I_j(\varphi) = e\mathcal{N}_j\Delta \sin \frac{\varphi}{2} \tanh \left(\frac{\Delta \cos \frac{\varphi}{2}}{2T} \right), \quad (28)$$

This is identical to the result derived by Kulik and Omel'yanchek (KO).¹⁶⁾ We next consider the weak coupling limit of $\Delta_0 \gg \Gamma_j$. In the low-temperature regime of $\Delta \gg \Gamma_j \gg T$, we can ignore all terms in the parentheses except for Δ^2 , and obtain²³⁾

$$I_j(\varphi) = e\mathcal{N}_j\Gamma_j \sin \frac{\varphi}{2} \tanh \left(\frac{\Gamma_j \cos \frac{\varphi}{2}}{2T} \right). \quad (29)$$

When $T_c \gtrsim T$, there holds $T \gg \Gamma_j, \Delta$ which enables us to retain only ω_n^4 in the denominator. We thus obtain

$$I_j(\varphi) = e\mathcal{N}_j \frac{\Gamma_j^2 \Delta^2}{48T^3} \sin \varphi. \quad (30)$$

This T -dependence is qualitatively different from the KO result which yields $I(\varphi) = e\mathcal{N}\Delta^2(4T)^{-1} \sin \varphi$ near T_c .

To observe the T -dependence of the critical current $I_c^{(j)} \equiv \max_{\varphi} \{I_j(\varphi)\}$, we numerically calculate $I_c^{(j)}$ for several values of $r \equiv \Gamma_j/\Delta_0$ on the basis of eq. (27). The T -dependence of Δ is determined by the gap equation $1 = \lambda_{\text{int}} \int_0^{\epsilon_D} d\epsilon \tanh(\frac{\sqrt{\epsilon^2 + \Delta^2}}{2T})/\sqrt{\epsilon^2 + \Delta^2}$, where λ_{int} is the dimensionless interaction constant, and the Debye energy is chosen as $\epsilon_D/\Delta_0 = 200$. The critical current $I_c^{(j)}$ normalized by $I_0^{(j)} \equiv e\mathcal{N}_j\Delta_0$ is shown in Fig. 2 as a function of T/T_c for $r = 0.2, 1.0, 5.0$, and $r \rightarrow \infty$ at which the KO result is reproduced. Note that $I_c^{(j)}/I_0^{(j)}$ does not depend on j . We observe that $I_c^{(j)}$ is a concave function of T at $r \rightarrow \infty$, while it crosses over to a convex function with decreasing r . Such a convex T -dependence was not observed in the previous study⁹⁾ based on an energy-independent effective pair potential model. The coupling strength Γ_j crucially affects the T -dependence of the critical current.

Let us finally evaluate the critical current at $T = 0$. As an intermediate step, we derive a convenient analytic formula by approximating the ω_n -dependence of the denominator of eq. (27) as $2\Gamma_j\sqrt{\Delta^2 + \omega_n^2} \approx 2\Gamma_j\Delta$. This is justified either in the low-temperature limit of $T_c \gg T$ for an arbitrary Γ_j , or in the strong and weak coupling limits for an arbitrary T . Performing the summation over ω_n in terms of a contour integral, we obtain

$$I_j(\varphi) = e\mathcal{N}_j \frac{\Gamma_j^2 \Delta^2 \sin \varphi}{\sqrt{E_+(\varphi)E_-(\varphi)}} \left[\frac{\tanh \left(\frac{E_+(\varphi) - E_-(\varphi)}{4T} \right)}{E_+(\varphi) - E_-(\varphi)} - \frac{\tanh \left(\frac{E_+(\varphi) + E_-(\varphi)}{4T} \right)}{E_+(\varphi) + E_-(\varphi)} \right], \quad (31)$$

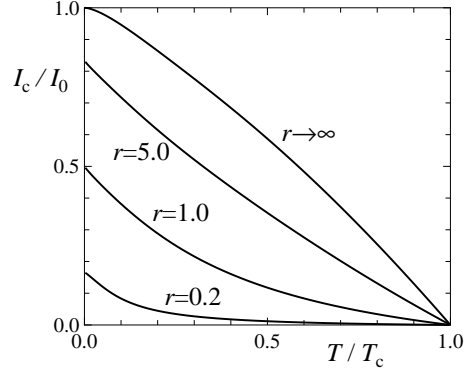


Fig. 2. Temperature dependence of the normalized critical current $I_c^{(j)}/I_0^{(j)}$ for $r = 0.2, 1.0, 5.0$, and $r \rightarrow \infty$, where $r \equiv \Gamma_j/\Delta_0$.

where $E_{\pm}(\varphi) = [(\Delta + \Gamma_j)^2 \pm 2\Gamma_j\Delta \cos(\varphi/2)]^{1/2}$. One can verify that eq. (31) reproduces the correct asymptotic behaviors, eqs. (28)-(30), in the corresponding limits. Note that eq. (31) is maximized at $\varphi = \pi \pmod{2\pi}$ in the limit of $T \rightarrow 0$. The critical current is determined as $I_c^{(j)} = e\mathcal{N}_j\Gamma_j\Delta_0/(\Delta_0 + \Gamma_j)$, which yields

$$I_c^{(1)} = e \frac{2\mu W}{\pi\gamma} \frac{\Gamma\Delta_0}{\Delta_0 + \Gamma} \quad (32)$$

for the monolayer, and

$$I_c^{(2)} = e \frac{2\mu W}{\pi\gamma} \sqrt{\frac{\gamma_1}{\mu}} \frac{\frac{\Gamma}{2}\Delta_0}{\Delta_0 + \frac{\Gamma}{2}} \quad (33)$$

for the bilayer cases. We see that $I_c^{(1)}$ is proportional to μ , which is consistent with the result reported in ref. 4, while $I_c^{(2)}$ is proportional to $\sqrt{\mu}$. Roughly speaking, the critical current in the bilayer case is greater than that in the monolayer case by a factor of $\sqrt{\gamma_1/\mu}$.

In summary we have proposed a model for a planar Josephson junction of graphene, and derived a general expression for the Josephson current at moderate doping in the quasiclassical Green's function approach. Much emphasis has been on the behavior of the Josephson current in the short-junction limit in monolayer and bilayer graphene junctions. It was demonstrated that the coupling strength crucially affects the temperature dependence of the critical current in an unexpected manner. This should be regarded as a characteristic feature of the planar junction. We have also shown that the chemical-potential dependence of the critical current qualitatively differs in the monolayer and bilayer cases. Finally we point out that our argument can be extended to a multilayer case.²⁰⁾ Such an extension will be reported elsewhere.

Acknowledgment

This work was supported in part by a Grant-in-Aid for Scientific Research (C) (No. 21540389) from the Japan Society for the Promotion of Science.

References

- 1) K. S. Novoselov, A. K. Geim, S. V. Morozov, D. Jiang, Y. Zhang, S. V. Dubons, I. V. Grigoriva, and A. A. Firsov: *Science* **306** (2004) 666.
- 2) A. H. Castro Neto, F. Guinea, N. M. R. Peres, K. S. Novoselov, and A. K. Geim: *Rev. Mod. Phys.* **81** (2009) 109.
- 3) K. Wakabayashi: *J. Phys. Soc. Jpn.* **72** (2003) 1010.
- 4) M. Titov and C. W. J. Beenakker: *Phys. Rev. B* **74** (2006) 041401.
- 5) A. G. Moghaddam and M. Zareyan: *Phys. Rev. B* **74** (2006) 241403.
- 6) J. González and E. Perfetto: *Phys. Rev. B* **76** (2007) 155404.
- 7) A. M. Black-Schaffer and S. Doniach: *Phys. Rev. B* **78** (2008) 024504.
- 8) M. Hayashi, H. Yoshioka, and A. Kanda: *Physica C* **470** (2010) S846.
- 9) I. Hagymási, A. Kormányos, and J. Cserti: *Phys. Rev. B* **82** (2010) 134516.
- 10) H. B. Heersche, P. Jarillo-Herrero, J. B. Oostinga, L. M. K. Vandersypen, and A. F. Morpurgo: *Nature* **446** (2007) 56.
- 11) X. Du, I. Skachko, and E. Y. Andrei: *Phys. Rev. B* **77** (2008) 184507.
- 12) C. Ojeda-Aristizabal, M. Ferrier, S. Guéron, and H. Bouchiat: *Phys. Rev. B* **79** (2009) 165436.
- 13) H. Tomori, A. Kanda, H. Goto, S. Tanaka, Y. Ootuka, and K. Tsukagoshi: *Physica C* **470** (2010) 1492.
- 14) W. L. McMillan: *Phys. Rev.* **175** (1968) 537.
- 15) A. V. Svidzinskii, T. N. Antsygina, and E. N. Bratus: *Sov. Phys. JETP* **34** (1972) 860.
- 16) I. O. Kulik and A. N. Omel'yanchuk: *Sov. J. Low Temp. Phys.* **4** (1978) 142.
- 17) J. C. Slonczewski and P. R. Weiss: *Phys. Rev.* **109** (1958) 272.
- 18) P. R. Wallace: *Phys. Rev.* **71** (1947) 622.
- 19) E. MacCann and V. I. Fal'ko: *Phys. Rev. Lett.* **96** (2006) 086805.
- 20) Y. Takane: *J. Phys. Soc. Jpn.* **79** (2010) 124706.
- 21) G. Eilenberger: *Z. Phys.* **214** (1968) 195.
- 22) A. I. Larkin and Yu. N. Ovchinnikov: *Sov. Phys. JETP* **28** (1969) 1200.
- 23) A. F. Volkov, P. H. C. Magnée, B. J. van Wees, T. M. Klapwijk: *Physica C* **242** (1995) 261.
- 24) A. Furusaki, H. Takayanagi, and M. Tsukada: *Phys. Rev. B* **45** (1992) 10563.